THE ASTROPHYSICAL JOURNAL, 252:653–667, 1981 January 15

Z CHAMAELEONTIS: EVIDENCE FOR AN ECCENTRIC DISK DURING SUPERMAXIMUM?[1]

NIKOLAUS VOGT[2]
European Southern Observatory
Received 1980 November 26; accepted 1981 July 6

ABSTRACT

Spectroscopic and photometric observations of the eclipsing dwarf nova Z Cha are presented. The main spectral features in quiescence are broad, double peaked emission lines of Hβ, Hγ, and Hδ, and narrow absorption lines of the higher-order Balmer series. The double structure of the emission profile is due to superposed narrow absorption which apparently arises in the line of sight through the outer, cooler parts of the disk. A radial velocity semiamplitude of 87 ± 14 km s^{-1} for the absorption lines was found. From the spectroscopic data, combined with published eclipse light curve characteristics, the principal system parameters of Z Cha were derived, in particular an orbital inclination $i=79°\pm2°$, stellar masses $M_1=0.85\pm0.15\ M_\odot$ and $M_2=0.17\pm0.05\ M_\odot$, binary separation, stellar radii, as well as size and location of the hot spot. Photoelectric high speed photometry, obtained during the 1978 March supermaximum, revealed partial eclipses, as well as superhumps whose period $P_s=0^d.07725$ exceeds the orbital period P_0 by 3.7%. Spectrograms during the same supermaximum resemble the quiescent spectrum, showing doubled emission for Hβ and Hγ and narrow absorption for the remaining Balmer lines. In addition, He II λ4686 and C III/N III λ4649 are present in emission. The radial velocity curve of the absorption lines shows similar phase and amplitude as in quiescence; however, their γ-velocities deviate strongly from the systemic velocity, showing variations of the order of ±200 km s^{-1} within 24^h. A similar effect is present in the published data of WZ Sge during its recent outburst. None of the previously suggested models for supermaxima and superhumps fits all observational constraints available now. Therefore, a new, consistent solution is suggested, implying an eccentric ring which surrounds the inner accretion disk during superoutburst. If the line of apsides of this elliptical ring rotates with the beat period (between P_0 and P_s), superhumps can be understood as arising from the maximal potential energy which is released in the stream/eccentric disk impact region ("superspot") near ring periastron. The ring could be formed by a suddenly enhanced mass flow through the inner Lagrangian point, transferring $\sim10^{24}$ g within $\sim10^3$ s.

Subject headings: stars: accretion — stars: dwarf novae — stars: eclipsing binaries — stars: individual

I. INTRODUCTION

Z Chamaeleontis is an outstanding dwarf nova: for several years it was the only known cataclysmic binary whose luminous components (white dwarf, central disk, and hot spot) are totally eclipsed by the red secondary. This configuration offers a unique possibility to study system dimensions, mass ratio, luminosity contributions of the different components, and, last but not least, location and nature of the dwarf nova outburst. Z Cha was discovered as an eclipsing binary by Mumford (1969), but the first crucial photoelectric observations with high time resolution in quiescence and during outburst were obtained by Warner (1974). They leave no doubt that the eruption energy is released near the white dwarf in the central part of the disk. Subsequently, several investigations were published on possible outburst mechanisms (Bath *et al.* 1974) and system parameters (Bailey 1979; Fabian *et al.* 1979; Smak 1979; Ritter 1980). Bailey (1979) added further photoelectric high speed observations in quiescence and showed that the white dwarf ingress and egress times define a very accurate long-term ephemeris. Two further dwarf novae with similar eclipse characteristics were detected recently: OY Car (Vogt 1979*a*) and HT Cas (Patterson 1978).

The spectrum of Z Cha in quiescence was described for the first time by Whelan, Rayne, and Brunt (1979), reporting doubled emission lines of H and He I. A more detailed presentation of these data is given by Rayne and Whelan (1981), who suggest that the emission line doubling is influenced by absorption effects. The varia-

[1]Based on observations collected at the European Southern Observatory, La Silla, Chile.

[2]Dedicated to Professor Dr. Friedrich Becker, my first tutor in astronomy, on the occasion of his 80th birthday.

tions of the Hα emission profile during an eclipse confirm that the disk rotates progradely, with velocities faster near the center than in the outer parts. Spectroscopic observations of Z Cha during outburst have not been published so far.

Z Cha belongs to the important SU UMa subgroup of dwarf novae which are characterized by rare semiperiodic supermaxima apart from the more frequent short eruptions (Vogt 1980). One supermaximum of Z Cha took place toward the end of March in 1978 and enabled the author to obtain photoelectric high-speed photometry as well as spectra with sufficient high time resolution to resolve the orbital phases. The data later were completed by spectroscopic observations during quiescence, which are described in § II (including some consequences on the model parameters of Z Cha). The outburst observations are given in § III. Their consistency with previously suggested models is investigated in § IV, leading to a new superoutburst scenario which is compatible with all known observational properties of SU UMa type dwarf novae.

II. Z CHA IN QUIESCENT STATE

a) *Spectroscopy*

Spectroscopic observations of Z Cha in quiescence were obtained in 1978 June 11–13 with the ESO 3.6 m telescope, using the Boller and Chivens spectrograph in the Cassegrain focus and the Carnegie image tube (two-stage, magnetically focused, S-20 spectral response). The dispersion was 114 Å mm^{-1}, the useful spectral range 3700–6500 Å. The typical exposure time (on baked IIIa-J plates) was between 15 and 20 minutes. Up to nine spectra could be collected at the same plate, which permitted one to minimize the time lost between subsequent exposures. Figure 1 shows the tracing of a typical spectrogram in quiescence. The most prominent features are the Balmer lines in broad emission, superposed by a narrow central absorption. This absorption simulates a double emission peak for Hβ, a well known feature of

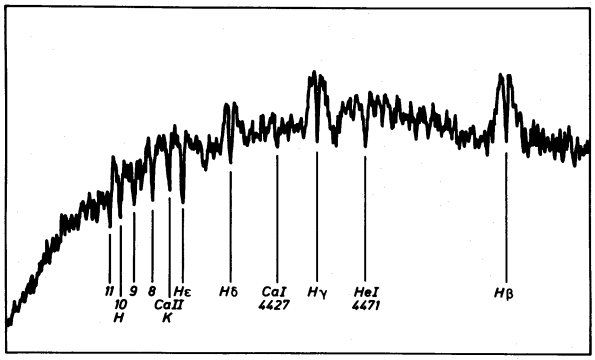

FIG. 1.—Density tracing of spectrum 449C in quiescence

cataclysmic binaries with high orbital inclination. Hγ and Hδ reveal an absorption core well below the stellar continuum, and for Hε to H11 the emission becomes nearly invisible, leaving only narrow, relatively deep absorption lines. In addition to Hydrogen, some lines of He I, Ca I, and Ca II are present in absorption. The mean total width of the Hβ, Hγ, and Hδ emission, measured at continuum level, is 4600 ± 100 km s^{-1}; the peak-to-peak separation 1460 ± 50, 1650 ± 50, and 2210 ± 90 km s^{-1} for Hβ, Hγ, and Hδ, respectively. Overall spectral features, line width, and peak-to-peak separation are similar to those of Whelan, Rayne, and Brunt (1979) and Rayne and Whelan (1981).

The radial velocities were measured with the modified Zeiss Abbé comparator of the La Silla Observatory which works on the same principle as a Grant machine. It turned out that only the emission peaks of Hβ and Hγ reveal reliable velocity values, which are listed in Table 1 (columns E^- and E^+). The velocities of the narrow absorption lines could be measured with higher accuracy. All Balmer lines from Hβ to H10, as well as the Ca II K line, gave coinciding results and were used for the average velocities listed in Table 1 under *A*. The typical mean error of the average absorption velocity is ± 22 km s^{-1}.

Figure 2 shows the radial velocities of emission and absorption components versus the orbital phase according to Bailey's (1979) ephemeris. Only the absorption line velocities are accurate enough for deriving a reliable radial velocity orbit. A least squares sine fit results in a system velocity $\gamma = 0 \pm 9$ km s^{-1} and a semiamplitude $K_1 = 79 \pm 13$ km s^{-1}. Since the exposure time was about 20 minutes, i.e., 0.19 units of the orbital phase, a systematic correction of 10% had to be applied to the radial velocity amplitude in order to account for the unresolved velocity variations during the exposure. Therefore, the corrected semiamplitude is $K_1 = 87 \pm 14$ km s^{-1}.

The velocity minimum coincides with orbital phase 0.23 ± 0.05, which confirms that the radial velocity variation is due to the orbital motion of the primary component in the binary system. The mean displacement of the emission peaks from the fitted absorption curve is -786 ± 38 and $+791 \pm 26$ km s^{-1}, respectively. No attempt was made to fit the emission peak velocities to a sine curve because of their large scatter. However, the absorption velocity curve fits also the emission peak values when applying the corresponding mean displacement (Fig. 2). Application of the *F*-test to the standard deviations from these curves (as compared to the no-variability hypothesis) reveals probabilities of >95% (E^-) and >99% (E^+) for the significance of periodic variations of the emission peaks parallel to those of the absorption lines.

The following interpretation of the above described facts is suggested: A hot, mainly continuum emitting

TABLE 1

SPECTROSCOPIC DATA OF Z CHAMAELEONTIS IN QUIESCENT STATE

PLATE	HJD −2,440,000 (mid-exposure)	BALMER RADIAL VELOCITY E^- (km s^{-1})	N^a	A (km s^{-1})	N^a	E^+ (km s^{-1})	N^a
444A ...	3671.4978	−762	2	−25	8	665	2
445A ...	3671.5193	...	...	+101	7	...	...
C	3671.5360	...	...	−59	6	788	1
E	3671.5502	−680	2	−86	7	628	1
G ...	3671.5652	−748	2	−16	8	814	2
449A ...	3672.4912	−707	2	+96	8	918	1
B	3672.5037	−686	1	+48	8	...	...
C	3672.5158	−995	1	−58	8	630	1
D ...	3672.5276	−825	2	−52	8	795	1
E	3672.5398	−830	2	−19	8	756	2
F	3672.5519	−608	2	+39	8	918	2
G ...	3672.5644	−664	2	+73	8	951	1

[a] N = Number of stellar lines used for the radial velocity determination.

central region of the disk, in vicinity of the white dwarf, is seen through a cooler outer disk portion which, in its entire extension, contributes to the Balmer emission. Only in the line of sight and in the transition zone from optically thin to the optically thick disk layers are the conditions appropriate to form absorption lines, which are narrow because they arise from tangentially orbiting material at a certain distance from the mass center. The Balmer decrement of the emission is steeper than that of the absorption; the latter, therefore, is dominant in the higher order members of the Balmer series. The radial velocities of emission and absorption components show parallel variations with orbital phase because they all follow the orbital motion of the primary. In particular, the observed peak-to-peak separation in the emission profile is result of this superposition, depending on width and relative strength of emission and absorption, and is not directly related to the disk rotation.

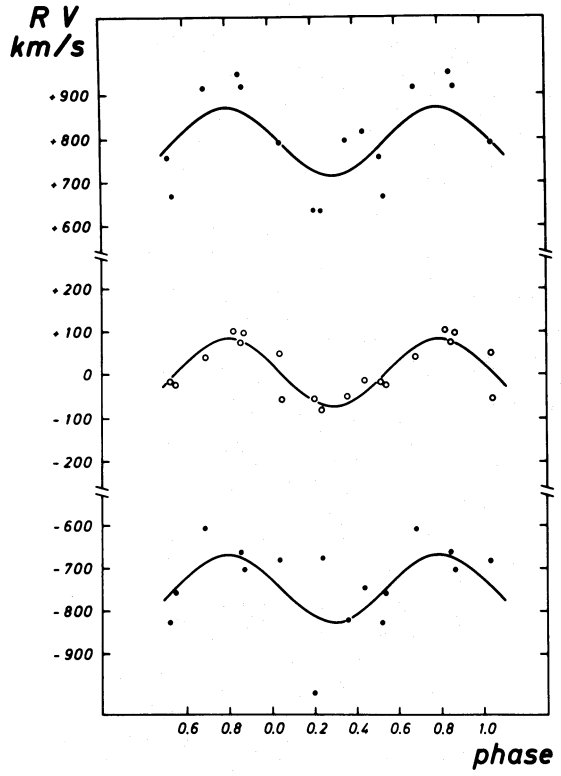

FIG. 2.—Radial velocity variations of the Balmer lines versus orbital phase in quiescence. *Dots*, emission peaks; *open circles*, absorption lines. The absorption line velocities were fitted to a least-squares sine curve (*solid line*), which is also drawn through the emission velocities, applying the proper displacement.

b) Determination of the Physical Parameters

The Roche model of cataclysmic binaries gives a well known relation between the relative radius of the secondary R_2/A (in units of the separation A between the mass centers) and the mass ratio $q=M_1/M_2$. This relation (here calculated in Paczyński's 1971 approximation) can be compared to expected radii of main sequence secondaries, according to the mass-radius relation of the lower main sequence (Grossman, Hayes, and Graboske 1974), which results in $M_2=0.17\ M_\odot$ for the secondary of Z Cha, if it is a main sequence star.

The observed width of the primary eclipse (344.4 s according to Bailey 1979) reveals a unique relation between q and orbital inclination i (e.g., eq. [8] in Ritter 1980) which is shown in the upper margin of Figure 3. Essentially the same relation is given by Bailey (1979) and by Fabian *et al.* (1979). Figure 3 contains the observed relative radius R_1/A of the primary based on the mean duration (40 s according to Bailey 1979) of its ingress and egress (cf. eq. [16] in Ritter 1980). This is compared to the expected R_1/A values for white dwarfs between 0.6 and 1.0 $M_\odot$ whose radii obey the

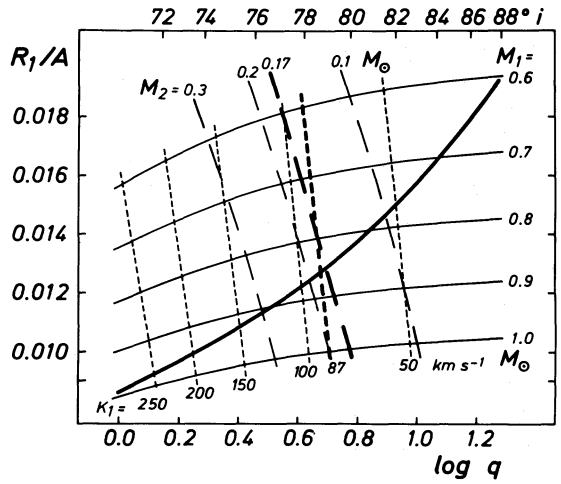

FIG. 3.—Radius R_1 of the primary (in units of the binary separation A), as derived from ingress/egress duration and eclipse width, vs. mass ratio q (*broad solid line*). The upper scale denotes the orbital inclination i as derived from the width of the primary eclipse. The narrow solid lines refer to relative radii as expected for various white dwarfs (with $0.6 \leq M_1 \leq 1.0\ M_\odot$) which obey the mass-radius relation of Kippenhahn and Thomas (1965). Secondary masses M_2 between 0.1 and 0.3 $M_\odot$ are shown as long dashes; the main sequence case ($M_2 = 0.17\ M_\odot$) is indicated broader. The short dashed lines correspond to radial velocity semiamplitudes K_1 of the primary, between 50 and 250 km s^{-1}; a broader line indicates the observed value ($K_1 = 87$ km s^{-1}). The most probable physical parameters of Z Cha are expected near the intersection of the three broad lines.

mass-radius relation of Kippenhahn and Thomas (1965), while A is given by the third Kepler law. Lines of constant secondary masses between 0.1 and 0.3 $M_\odot$, and of expected radial velocity semiamplitudes K_1 of the primary (cf. eq. [10] in Warner 1976) are shown as well. The observed R_1/A line coincides with the main sequence status of the secondary ($M_2 = 0.17\ M_\odot$) and with the observed K_1 value (87 km s^{-1}) for $M_1 = 0.85\ M_\odot$ ($q = 5.0$).

Which systematical errors could affect this result? The observational errors are insignificant compared to the uncertainties which arise in the interpretation of the eclipsed object. In principle, a comparison of the observed R_1/A values with the theoretical mass-radius relation is valid only if the primary is actually a normal white dwarf. In this case, we always should observe identical ingress and egress durations. However, their significant variability as reported by Smak (1979) could be an indication that the primary radius is variable, i.e., that the eclipsed body is actually a small luminous central part of the disk in which the white dwarf is embedded. In this case, the observed R_1 is larger than the white dwarf radius; so derived M_1 values are lower mass limits.

A second correction has to be applied when reducing the observed ingress and egress phases to the true geometrical phases of contact: A spherical or elliptical object with limb darkening will produce a gently rounded light curve near the contacts, which may be masked by photon statistics and flickering. The apparent contact times are mainly based on the steep, linear portion of the light curves, which tends to underestimate the duration of ingress and egress. Patterson (1978) applied a correction of 24% in a similar case (HT Cas). Such a correction would move the observed R_1/A relation in Figure 3 toward 24% larger radii, i.e., to $M_1 \approx 0.7\ M_\odot$ for $M_2 = 0.17\ M_\odot$. Fortunately, both uncertainties partly compensate each other. Therefore, the situation as displayed in Figure 3 may be the best approximation to reality.

The physical parameters of Z Cha are listed in Table 2; their errors reflect mainly uncertainties in the interpretation. In addition, the radius R_{HS} of the hot spot, its distance d_{HS} to the primary (in units of A), and its position angle α were derived. The error range for these parameters is due to the observed variation in phase and duration of the hot spot eclipse, according to Smak (1979). In contrast to the situation found for OY Car (Vogt *et al.* 1981), the hot spot of Z Cha seems to maintain its angle α, but varies its position due to changes of the disk radius.

c) *Discussion*

The above parameters of Z Cha essentially agree with those of Smak (1979), who analyzed Warner's (1974) and Bailey's (1979) eclipse light curves, and derived $4 \leq q \leq 9$; this implies $M_1 \gtrsim 1\ M_\odot$ if the secondary is a main sequence star. Smak's and the present study are, however, in conflict with the Fabian *et al.* (1979) constraint $0.5 \lesssim q \lesssim 1.5$ which is based on a comparison between observed and theoretical hot spot ingress phases, the latter ones predicted due to gas-dynamical calculations of stream position and disk size. But Figure 2 in Fabian *et al.* (1979) demonstrates that the total variation in the theoretically predicted phase of the hot spot ingress is from -115 to -64 s (for $q = 1$ to 5, respectively.) Exactly the same variation was found by Smak (1979) when comparing Warner's (1974) with Bailey's (1979) eclipse light curves! Since the binary cannot have

TABLE 2

PHYSICAL PARAMETERS OF Z CHAMAELEONTIS

$i = 79° \pm 2°$
$M_1 = 0.85 \pm 0.15\ M_\odot$
$M_2 = 0.17 \pm 0.05\ M_\odot$
$A = (5.2 \pm 0.3) \times 10^{10}$ cm
$R_1 = (6.7 \pm 1.5) \times 10^8$ cm
$R_2 = (1.32 \pm 0.15) \times 10^{10}$ cm
$d_{HS}/A = 0.31 \pm 0.03$
$R_{HS}/A = 0.023 \pm 0.004$
$\alpha = 30°.5 \pm 1°$

changed its mass ratio between both epochs, we conclude that other factors than the mass ratio will have stronger influence on the observed hot spot ingress phase, and that the Fabian *et al.* (1979) method is not adequate for deriving mass ratios.

Another study of Z Cha was recently published by Ritter (1980). His results $M_1=0.35\ M_\odot$, $q=2.2$ differ also from the values derived here. Since his input parameters are essentially the same (although of lower accuracy: he used only one eclipse light curve!), his method has to account for the large difference in the binary parameters. Indeed, he assumes that the separation of the double peaks in the Balmer emission line profile is identical with the projected rotation velocity of the outer rim of the disk. The observational evidence given above in § II*a* disproves Ritter's approach. Disk rotation actually is not responsible for the peak separation in the profiles.

Z Cha is not the only ultrashort period cataclysmic binary with a relatively large primary mass. Its northern counterpart HT Cas has $M_1\geq 0.8\ M_\odot$ (Patterson 1978); Vogt *et al.* (1981) derived $M_1=0.95\ M_\odot$ and $q=6.8$ for OY Car. Breysacher and Vogt (1980) found $M_1=1.4\ M_\odot$, $q=7.4$ for the X-ray binary and dwarf nova EX Hya (which reveals partial eclipses). The two noneclipsing ultrashort-period dwarf novae VW Hyi and WX Hyi also have primary masses $\sim 0.8\ M_\odot$ and large mass ratios of $q\approx 6$ (Schoembs and Vogt 1980*b*). Since these studies were carried out independently, applying different methods, their concordant results $M_1\approx 1\ M_\odot$ and $4\geq q\geq 9$ for all ultrashort-period dwarf novae (with the possible exception of WZ Sge) deserves certain confidence. This implies, among other consequences, a conflict with Webbink's (1979) hypothesis that the observed period gap between 2^h and 3^h reflects the mass discontinuity between helium white dwarfs ($0.21\leq M\leq 0.46\ M_\odot$) and carbon-oxygen white dwarfs ($0.56\leq M\leq 1.4\ M_\odot$). Since the primary masses of most (if not all) cataclysmic binaries turn out to be near $1\ M_\odot$, a different mechanism has to account for the period gap.

III. Z CHA DURING SUPERMAXIMUM

The supermaximum of 1978 March/April lasted for a total of about 15^d and was fairly well monitored by visual observers of the Royal Astronomical Society of New Zealand (Bateson 1980). Figure 4 shows a smoothed light curve based on visual estimates. The arrows indicate the approximate epochs of spectroscopic and photometric observations carried out at ESO in La Silla, and presented in this section.

a) Photometry

The photoelectric photometry of Z Cha consists of a 4.5 hour run in 1978 March 29/30, and two 2-hour runs in both subsequent nights, always with 3 s time resolution. The first run was obtained at the ESO 3.6 m telescope, using the Behr three-channel photometer, whose dichroic filter system permits the simultaneous measurement of all three *UBV* channels. However, such a configuration cannot match the standard *UBV* system because of lacking overlap between the channels. A transformation of these data into the standard system was not possible. For the remaining two runs, obtained at the ESO 50 cm telescope, only a single channel photometer was available, and Z Cha was observed in Johnson *B*.

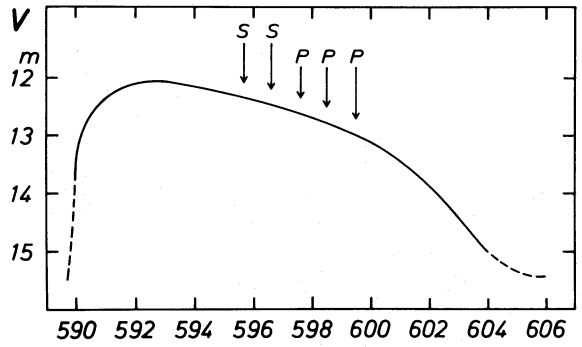

FIG. 4.—Smoothed light curve of the supermaximum of 1978 March/April, according to the records of the Royal Astronomical Society of New Zealand, Variable Star Section. The arrows indicate approximate time of spectroscopic (S) and photometric (P) observing runs at ESO. Abscissa is JD−2,443,000.

All high speed data were reduced to magnitude differences to the comparison star which was measured at beginning and end of each observing run (star 123 on the finding chart of Bateson, Jones, and Stranson 1966; the same star is identified as s by Bateson 1978). Photoelectric *UBV* standard photometry of this star in La Silla (ESO 50 cm telescope) revealed $V=12.29$, $B-V=0.66$, and $U-B=0.15$. In addition to the high speed photometry, single *UBV* measurements of Z Cha in three nights were obtained with the ESO 50 cm telescope. They are listed in Table 3.

The eclipse light curves resemble those of Warner (1974) in superoutburst state, revealing partial eclipses with a rounded minimum of slightly variable shape. The time of minimum was determined with the Pogson method and listed in Table 4. The $O-C$ deviations refer to Bailey's (1979) ephemeris. There is a weak tendency to positive values ($\langle O-C\rangle=(+15\pm 5)\times 10^{-5}$ days for

TABLE 3

PHOTOELECTRIC *UBV* PHOTOMETRY OF Z CHAMAELEONTIS DURING SUPERMAXIMUM

HJD	*V*	*B*−*V*	*U*−*B*
2,443,596.7045 ...	12.96	0.03	−0.66
2,443,598.5362 ...	13.00	0.05	−0.78
2,443,599.5619 ...	13.31	0.07	−0.67

TABLE 4

ECLIPSE DATA DURING SUPERMAXIMUM

E	Minimum HJD− 2,440,000	O−C (10^{-5} d)	Depth (mag) V	B	U	Half-Width (minutes) V	B	U	Maximal Gradient (mag minute^{-1}) Decline V	B	U	Rise V	B	U
44702[a]	3594.9484	+46	1.8:	...	...	6.5:	...	...	...	...	...	...	...	...
44738	3597.63000	+9	1.44	1.62	1.74	5.31	5.01	4.82	0.368	0.458	0.501	0.412	0.495	0.545
44739	3597.70459	+18	±6	±2	±3	±9	±6	±5	±5	±8	±13	±18	±13	±6
44740	3597.77903	+12	...	...		...	...	...	...	...	...	...	...	...
44751	3598.59875	+35		1.3			4.91			0.403			0.392	
44767	3599.64142	+3		1.43			5.09			0.416			0.405	

[a]Derived from visual observations Bateson (1980).

the five photoelectrically observed eclipses) which seems to be confirmed by one visual eclipse observation (also listed in Table 4). Bailey (1979) found $\langle O-C\rangle=(+46\pm12)\times10^{-5}$ days for Warner's (1974) six superoutburst eclipses. Bateson (1978) listed 29 eclipse times observed visually during five different supermaxima, which give mean values of $\langle O-C\rangle=+57$, $+162$, $+129$, $+299$ and $+29\times10^{-5}$ days (with a typical mean error of $\pm25\times10^{-5}$ days for each of these values). Although this result may partly be affected by the lower accuracy and possible unknown systematic errors in the visual estimates, it proves the preference for positive $O-C$ values, and indicates also a significant variability from outburst to outburst.

Table 4 contains additional well defined parameters of the eclipse light curve, i.e., the depth (taking as reference the magnitude averaged at phases -0.1 and $+0.1$), the eclipse width halfway to minimum, and the maximal gradients, corresponding to the quasi-linear portion of decline and rise. For the first run, only mean parameter values from three observed eclipses are given. The light curve shape shows a significant color dependence, revealing the deepest, narrowest eclipses with the largest gradient in the ultraviolet. In the two subsequent runs, the eclipse amplitude and gradients had slightly diminished while the width remained unchanged. The extensive photometry during a supermaximum of OY Car (Krzeminski and Vogt 1981) demonstrates that all these eclipse parameters vary with the time elapsed after maximum, with superhump phase, and with bandpass. Unfortunately, the limited amount of data available for Z Cha does not permit such an analysis.

Remarkable variations of the light curve shape outside the eclipses are present in the photoelectric data. The first run reveals a light maximum at phase ~0.3, the second run at phase ~0.8. The third run shows nearly constant brightness outside the eclipse, with a weakly pronounced maximum at phase ~0.2. The changing phase shifts of the light maxima are in complete analogy to the superhumps of other noneclipsing SU UMa stars (e.g., VW Hyi: Haefner, Schoembs, and Vogt 1979). Table 5 contains four moments of superhumps, present in the three photoelectric observing runs, and two additional ones ($E=0,1$) which were derived from Bateson's (1980) visual Royal Astronomical Society of New Zealand data just after outburst maximum, when the superhump amplitude was especially large (~0.5 mag). The following ephemeris could be derived from the six moments of superhumps:

$$\text{HJD (superhump max.)}=2{,}443{,}593.8676+0.07725\,E. \quad (1)$$
$$\pm10 \qquad \pm2$$

In Warner's (1974) two observing runs obtained during an earlier supermaximum (1973 January, his Figs. 4 and 5) three superhumps can be recognized whose times are also listed in Table 5. They are consistent with a superhump period of $0^d.0774\pm0^d.0002$, identical with (1). The superhump period of Z Cha exceeds the orbital

TABLE 5

SUPERHUMPS OF Z CHAMAELEONTIS

Date of Observation	E	HJD −2,440,000	O−C (10^{-4} d)
1978 March (this paper).....	0[a]	3593.868	+4
	1[a]	3593.944	−9
	49	3597.6528	−1
	50	3597.7305	+4
	61	3598.5819	+21
	74	3599.5824	−17
1973 January (Warner 1974) ...	0	1691.4398	−14
	1	1691.5202	+16
	12	1692.3697	−1

[a]Derived from visual observations (Bateson 1980).

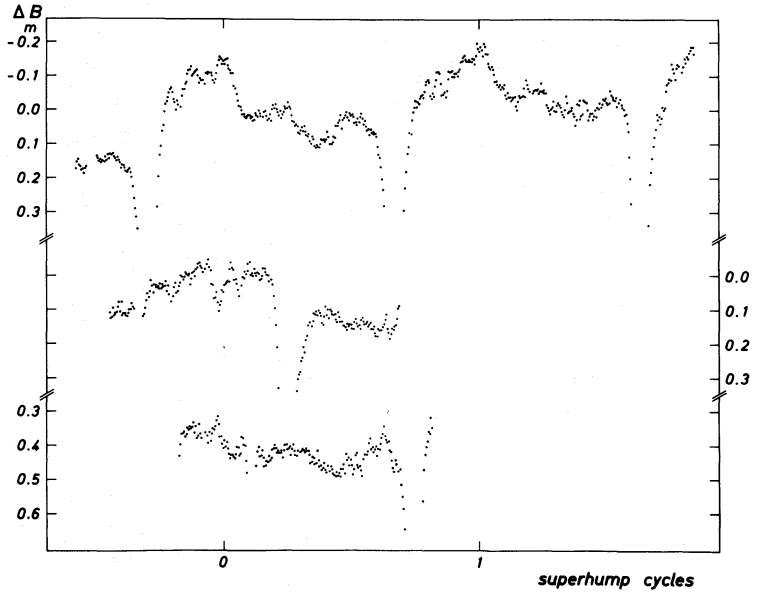

FIG. 5.—Photoelectric light curves during supermaximum (B mag difference between variable and comparison star) in 1978 March 29/30 (*top*), March 30/31 (*middle*), and March 31/April 1 (*bottom*). Only the upper portions of the eclipse light curves are shown. The time is given in cycles of elements (1), referring to $E=49$, 61, and 74, respectively, for cycle 0 in the three runs.

period by 3.7%, in close analogy to VW Hyi (Haefner, Schoembs, and Vogt 1979) and WX Hyi (Schoembs and Vogt 1981).

The light curves of Z Cha (outside the eclipses) in the three photoelectric observing runs during the March 1978 supermaximum are shown in Figure 5. The relatively small superhump amplitude ($\lesssim$0.2 mag) is consistent with the advanced outburst stage at which the photoelectric data were obtained.

b) *Spectroscopy*

Spectrograms of Z Cha were taken in the two nights preceding the first photometric run (cf. Fig. 4), with the ESO 3.6 m telescope. Instrument, equipment, and dispersion were identical to those described in § II*a*. Two spectrograms were obtained in March 27/28; the remaining 17 spectra cover nearly two orbital cycles in March 28/29. Typical exposure times range from 3 to 5 minutes; the time resolution was about 6 minutes.

Figure 6 shows tracings of five exemplary spectrograms at different orbital phases. The strongest emission lines present are He II λ4686, C III/N III blend at λ4649, and the lower-order members of the Balmer series (Hα to Hγ, marginally Hδ). Most of the Balmer emission profiles are double peaked due to a narrow central absorption which becomes more and more dominant for the higher-order Balmer lines. In addition, Ca II K appears in absorption.

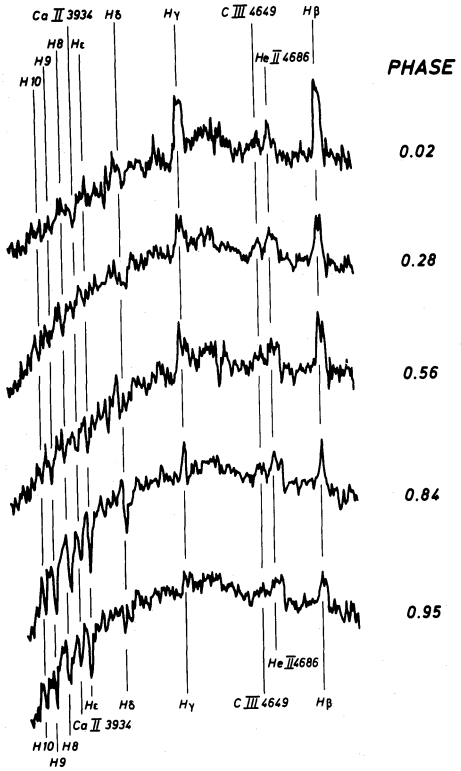

FIG. 6.—Density tracing of several spectrograms during supermaximum, corresponding to different orbital phases (plates 369G, 370A, 370F, 369D, and 369F from top to bottom).

TABLE 6

SPECTROSCOPIC DATA ON Z CHAMAELEONTIS DURING THE 1978 MARCH SUPERMAXIMUM

PLATE	HJD −2,440,000 (mid-exposures)	BALMER RADIAL VELOCITY E^- (km s^{-1})	N^a	A (km s^{-1})	N^a	E^+ (km s^{-1})	N^a
363A...	3595.7266	...		−213	6	465	2
B...	3595.7301	−825	3	−182	7	603	4
368A...	3596.6502	...		+434	6	872	1
369C...	3596.7191	−391	7	+401	5	...	
D...	3596.7237	−598	5	+341	6	...	
E...	3596.7277	−699	5	+372	7	...	
F...	3596.7318	−652	4	+286	7	...	
G...	3596.7370	...		...		790	1
H...	3596.7408	−655	4	+265	7	668	1
I ...	3596.7437	−616	4	+108	7	329	1
370A...	3596.7565	−748	3	+173	6	291	2
B...	3596.7605	−598	3	...		305	3
C...	3596.7646	−752	7	+253	5	186	2
D...	3596.7688	−757	6	+214	7	569	3
E...	3596.7729	−799	6	+222	7	658	3
F...	3596.7771	−683	5	+239	7	691	3
G...	3596.7812	−537	5	+310	8	609	2
H...	3596.7855	−472	6	+422	5	639	2
I ...	3596.7902	−483	6	+372	7	617	1

[a] N = Number of stellar lines used for the radial velocity determination.

Radial velocity measurements were carried out in the same way and with the same instrument as described above for the spectrograms of Z Cha in quiescence. Whenever possible, the blue and red emission peaks E^- and E^+ (mainly for Hβ, Hγ, and He II) as well as the absorption component A (here mainly confined to Hδ–H10 and Ca II K) were measured. The results for the Balmer lines are listed in Table 6. The periodic radial velocity variations of all three Balmer components are shown in Figure 7, together with a least squares sine fit for each component. Table 7 contains the results for the Balmer series (as shown in Fig. 7), for He II λ4686 and for Ca II K. The phase shifts of all radial velocity curves coincide within the error of determination, showing minimal velocities near $\phi_0 = 0.25$. The He II line turned out to be strong enough for radial velocity measurement only in the phase interval $0.39 \leq \phi_0 \leq 0.85$. Most spectra in this phase interval reveal two well defined He II emission peaks whose K and γ values were determined adopting the above phase shift.

The main results from the spectroscopic data presented here can be summarized as follows:

i) There is a certain similarity between the spectra at supermaximum and in quiescence, which, in either case, permits one to distinguish between components E^-, A, and E^+ in the Balmer line profiles, the emission showing always a steeper decrement than the absorption.

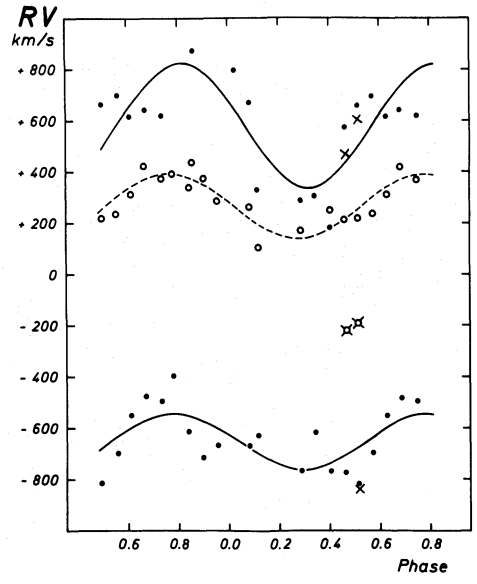

FIG. 7.—Radial velocity variations of the Balmer lines vs. orbital phase during supermaximum. *Dots*, emission peaks (E^-, E^+) in March 28/29; *open circles*, absorption lines (A) in March 28/29; *crosses*, emission peaks in March 27/28; *crossed open circles*, absorption lines in March 27/28. The components E^-, A, and E^+ in March 28/29 were fitted independently to least-squares sine curves which are shown by solid lines (E^-, E^+) and a dashed line (A).

TABLE 7

RADIAL VELOCITY VARIATIONS OF Z CHAMAELEONTIS IN 1978 MARCH 28/29

SPECTRAL LINES	E^-			A			E^+		
	K	γ	N^a	K	γ	N^a	K	γ	N^a
Balmer series	106±34	−639±24	15	122±18	+267±13	15	240±56	+578±39	13
He II 4686	114±33	−579±21	7	...	...	...	99±38	+907±24	7
Ca II K	...	...		147±51	+254±35	16		...	

[a] N = number of spectrograms.

However, the emission is narrower at superoutburst, its double structure is not so clearly defined, and the mean peak-to-peak separation (1217±52 km s^{-1}) is smaller than at quiescence (1577±46 km s^{-1}). On the other hand, the average between red and blue emission peak velocity (−30±52 km s^{-1}) agrees with that observed in quiescence (+2±46 km s^{-1}) and with the γ-velocity of the absorption lines in quiescence (γ_0=0±9 km s^{-1}). The presence of the high excitation emission (He II, C III/N III) is restricted to the supermaximum stage.

ii) In contrast to the behavior in quiescence, there is a significant spectral variation with orbital phase: The emission is strongest (relative to the continuum) during the eclipse and diminishes gradually at later phases. In the same way increases the strength of the Balmer absorption, which is absent during the eclipse and reaches its maximum near orbital phase ϕ_0=0.9 (in March 28/29), which corresponds to the superhump maximum (ϕ_s=0) in this night. The two spectra taken in the previous night (at $\phi_0 \approx 0.48$, $\phi_s \approx 0.06$) show slightly stronger absorption lines than those of $\phi_0 \approx 0.5$ in March 28/29. This could be an indication that the maximum of the Balmer absorption coincides with the time of the superhump (ϕ_s=0), i.e., that the Balmer absorption strength varies parallel to the continuum intensity.

iii) The radial velocity semiamplitudes of the Balmer components E^- and A, of the Ca II K line, and of both He II emission peaks agree, within the error of determination, with the value derived from the Balmer absorption in quiescence.

iv) All radial velocity curves show their minimum near orbital phase ϕ_0=0.25, which is expected if the radiation sources responsible for the optical line spectrum are centered on the primary in quiescence as well as during superoutburst.

v) The γ-velocity of the Balmer absorption in March 28/29 (γ_{28}=+267±13 km s^{-1}) deviates from γ_0 at quiescence, as well as from the average of red and blue Balmer emission peaks, which is $\approx\gamma_0$. On the other hand, the average of red and blue He II emission peaks is +164±32 km s^{-1}. The Ca II K absorption line velocities coincide with γ_{28}. The relative large amplitude and enhanced scatter of the E^+ velocity curve (cf. Fig. 7) is probably a spurious effect, a consequence of the near coincidence of E^+ with the absorption lines in this night.

vi) The γ-velocity of the Balmer absorption, as determined in March 27/28 from the two available spectrograms (γ_{27}=−197±37 km s^{-1}), is different from γ_0 and from γ_{28} while the emission peak velocities coincide with those observed in March 28/29 (cf. Fig. 7). The time interval between both observations ($1^d.0$) is half of the beat period P_b=$2^d.1$ between P_0 and P_s; i.e., γ_{27} and γ_{28} may exemplify the extrema of the total γ-variation if this variation is periodic with P_b.

IV. MODELS OF SU URSAE MAJORIS TYPE SUPERMAXIMA

a) *Observed Properties*

Our present knowledge on the behavior of SU UMa stars is mainly based on photometric observations in quiescence and during outburst. The results recently were reviewed by Vogt (1980). Here just a short summary is given and completed by a few additional references.

Dwarf novae of the SU UMa type are characterized by two very distinct types of outbursts: the more frequent short eruptions which are not outstanding as compared to the outbursts of other dwarf novae, and the longer lasting and brighter supermaxima. The following facts are established for supermaxima:

i) During the rise branch no major peculiarities are present, as compared to any other dwarf nova eruption.

ii) Just after maximum periodic peaks, so-called superhumps, appear in the light curve which repeat with a period P_s exceeding the orbital period P_0 by a few percent. The superhump phenomenon apparently is not related to the orbital inclination. The amplitude of the superhumps decreases in the course of a supermaximum. P_0 and P_s are in the ultrashort-period domain ($\lesssim$2 hours).

iii) The linear and circular polarization is very small ($\lesssim$0.1%) during and just after supermaximum (Schoembs and Vogt 1980), as well as in quiescence (Knoechel and Vogt 1981). No periodic variations of the polarization with P_0 or P_s were found.

iv) Eclipsing SU UMa stars (Z Cha, OY Car) reveal partial eclipses during both types of outburst. $O-C$ is positive during supermaxima and seems to be modulated with the beat period P_b arising from P_0 and P_s. The eclipse depth gradually is increasing in the course of the outburst, but it is reduced if the superhump coincides with the eclipse (unpublished data on OY Car: Krzeminski and Vogt 1981).

v) Apart from Z Cha as presented here, only sparse information on spectra during supermaximum is available. VW Hyi and V436 Cen show very shallow and broad absorption (H, He I) at maximum (Vogt 1976; Whelan, Rayne, and Brunt 1979). During decline, VW Hyi reveals a featureless continuum or faint emission (Schoembs and Vogt 1981).

b) Comparison with WZ Sagittae

Outstanding in the outburst spectrum of Z Cha is the presence of relatively strong emission lines (which are narrower than in quiescent state), and of the higher-order Balmer series and Ca II K in narrow absorption. Most dwarf novae so far observed at outburst (including other SU UMa stars; cf. § IV*a*[v]) show a featureless continuum or shallow Balmer absorption lines which are considerably broader than the emission in quiescence. There is only one case which resembles Z Cha in this respect: WZ Sge, a dwarf nova with an extremely large cycle length of 33 years. At quiescence, WZ Sge does not undergo total eclipses of white dwarf and central disk (as Z Cha), but it shows a partial eclipse of the hot spot from which an orbital period $P_0 = 0^d.0566878455$ was derived (Robinson, Nather, and Patterson 1978). During its most recent outburst in 1978 December a superhump was detected whose period exceeds P_0 by 1% (Bohusz and Udalski 1979). Therefore, WZ Sge seems to share some properties with the SU UMa stars as described in the previous section.

The spectrum of WZ Sge during the 1978 outburst (Crampton, Hutchings, and Cowley 1979; Brosch, Liebowitz, and Mazeh 1980; Gilliland and Kemper 1980; Ortolani *et al.* 1980; Walker and Bell 1980) is essentially identical to that of Z Cha during supermaximum: Hα, Hβ, He II λ4686, and C III/N III λ4640–4650 appear in emission (mostly doubled), the higher-order Balmer lines, He I, and Ca II K in a relatively narrow absorption. Radial velocity studies were carried out independently by three groups; they all agree in a periodic variation of the absorption lines with period P_0 and with a semiamplitude $K \approx 150$ km s^{-1}, while the Hα and Hβ emission peaks remain stationary. However, the resulting γ-velocities of the Balmer absorption differ strongly from author to author, and, if sufficient coverage is available, from night to night. The authors attributed this effect to unknown systematic errors and ignored it in their discussion. On the other hand, this effect resembles the strongly variables γ-velocities found for the Balmer absorption of Z Cha in superoutburst. Based on the above hypothesis, that the γ-velocities vary with the beat period P_b (of P_0 and P_s: cf. § III*b*[vi]), all available γ data of WZ Sge in outburst were plotted versus beat phase ($P_b = 6^d.176$) in Figure 8. In spite of the incomplete coverage and the large scatter (which is expected from data of various authors, instruments, measuring methods, etc.) the data may indicate a periodic variation with P_b. A least-squares sine fit reveals a semiamplitude 103 ± 39 km s^{-1} and a mean system velocity of -18 ± 27 km s^{-1}, which coincides with the systemic velocity $\gamma_0 = -25 \pm 20$ km s^{-1} in quiescence (Krzeminski and Kraft 1964).

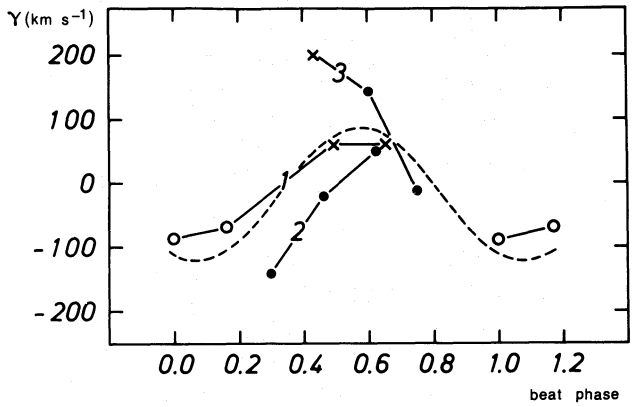

FIG. 8.—Observed Balmer absorption γ-velocities of WZ Sge vs. phase of the beat period ($6^d.176$) during the 1978 December eruption. *Open circles*, Crampton *et al.* (1979); *dots*, Gilliland and Kemper (1980); *crosses*, Walker and Bell (1980). The straight lines join subsequent observations within the same beat cycle. Beat phase 0 was chosen arbitrarily and coincides with Crampton *et al.*'s (1979) first observing run. Numbers 1 to 3 refer to the current number of beat cycles, and indicate the time sequence of the data. The dashed line shows a least-squares sine fit.

If this interpretation is correct, Z Cha would not be unique in showing a drifting γ-velocity in superoutburst. Tentatively one could conclude that narrow Balmer absorption and γ-variations with period P_b are properties of SU UMa type dwarf novae (here including WZ Sge) with high orbital inclination $i \lesssim 70°$.

The line spectrum characteristics depend strongly on i, in contrast to the continuum radiation (superhumps!).

c) Previous Suggested Models and their Criticism

Various models for superhumps and supermaxima have been suggested. Most of them, however, consider and explain only certain aspects of the observational data. The purpose of this section is to check the consistency of all previously suggested models, taking into account the new data of Z Cha and the other observed properties of SU UMa stars in supermaximum (§ IV*a*). The model of Papaloizou and Pringle (1978) can be immediately discarded since they consider P_s to be the orbital period. The radial velocity curves of VW Hyi

(Schoembs and Vogt 1981) and the data on Z Cha presented here disprove this assumption. Among the remaining models four types can be distinguished:

i) *Starspot on the Secondary (Vogt 1977; Haefner, Schoembs, and Vogt 1979)*

This model assumes that the superhumps are due to a bright spot temporarily present on the surface of the red secondary companion. The model predicts absorption lines whose radial velocity amplitude and phase shift correspond to the orbital motion of the secondary. The data on Z Cha, however, demonstrate that the entire line spectrum arises from radiation sources centered at the primary.

ii) *Strong Magnetic Field of the White Dwarf*

In these models the magnetic field is mostly of the white dwarf, which is suggested to rotate either with the superhump period P_s (Patterson 1979) or with the beat period P_b (Vogt 1979*b*). However, they give no convincing explanation for the presence of narrow absorption lines, although the slow γ-shifts at supermaximum are compatible with an extremely slow rotation of the white dwarf (Vogt 1979*b*). This, of course, causes serious theoretical objections. In addition, the absence of a significant linear or circular polarization in all stages of activity (cf. § IV*a*[iii]) is not in favor of such models since some similarity to AM Her type stars should be expected if strong magnetic fields are of great importance. This argument is also valid against Meyer's (1979) superhump model which suggests that magnetic flux tubes, which arise on the secondary's surface, connect with the disk and cause a hundredfold increase in the mass flow during supermaxima. In order to account for the observed superhump periods, a strongly asynchronous rotation of the secondary is required—a difficult assumption from the theoretical point of view.

iii) *Mass Transfer Variations through L_1*

These models are based on the idea that the dwarf nova eruptions, in general, are triggered by an enhanced rate of mass transfer due to dynamical instabilities in the secondary's envelope (Bath 1975). Subsequently, the superhumps are caused by periodic variations in the mass transfer rate, due to a very small eccentricity ($\sim 10^{-4}$) of the binary orbit (Papaloizou and Pringle 1979) or to a temporary alignment of several *g*-mode oscillations of an asynchronously rotating secondary (Vogt 1980). Both models fit to the photometric properties during supermaxima; however, they give no explanation for the spectroscopic results on Z Cha and WZ Sge, in particular the narrow Balmer absorption lines and the shifted γ-velocities.

iv) *The External Disk*

In this model, proposed by Gilliland and Kemper (1980) for WZ Sge and for SU UMa stars, the binary system is surrounded by an "excretion disk," i.e., a ring of gas, orbiting around the mass center at a distance of a few times the binary separation. A gas stream from one of the outer Lagrangian points hits the disk and forms a hot spot. Gilliland and Kemper (1980) show that the superhump phenomenon can be explained by the migration of this hot spot on a slightly inhomogeneous excretion disk. They also attribute the narrow absorption lines as arising from the hot spot whose observed radial velocity semiamplitude displays the projected Keplerian velocity of the external disk. However, there is no way to explain the shifting γ-velocity (with time scale $\sim P_b$) in this model. In addition, it is not clear how the narrow absorption lines of H and Ca II can arise in a hot spot, since the analogous spots at inner disks are characterized by a hot continuum and emission lines of high excitation. A third severe argument against Gilliland and Kemper's model is the disappearance of the absorption lines during eclipse, as clearly shown in Figure 6. This gives convincing evidence that the source of the absorption lines is eclipsed by the secondary and must, therefore, be located near the primary.

The models in groups (i), (ii), and (iv) seem to be inconsistent with the observational evidence available now. Only group (iii) may contain certain steps toward a consistent solution, which, however, must be completed taking into account the new spectroscopic data.

d) A Consistent Solution

The rather striking similarity of the line spectrum in quiescence and in outburst (cf. § III*b*[i]) apparently indicates that the physical configuration of the quiescent state is principally maintained during outburst. In particular, this is valid for the disk which, in both stages, seems to consist on a luminous, optically thick central part of high temperature, and a cooler, optically thin outer ring. This ring was considered as a source of the narrow Balmer absorption in quiescence (cf. § II*b*), and the most natural assumption would be to apply this model to the superoutburst state as well. However, the occurrence of partial eclipses indicates that the central, optically thick disk region is larger at outburst than in quiescence. The color behavior of the eclipses (cf. § III*a*) is compatible with a temperature increase toward the center. The narrow absorption lines arise—as in quiescence—in an outer ring surrounding the central disk. This general picture is easily compatible with amplitude, shape, and phase of the radial velocity curves (§§ III*b*[iii], III*b*[iv]) which mainly reflect the orbital motion of the primary. The disappearance of the absorption during the eclipse (§ III*b*[ii]) confirms that the absorption is actually formed in the line of sight toward

the central disk. Only the shifts of the γ-velocities (§§ IIIb[v] and IIIb[vi]) seem to be in disagreement with this model, at least if the material in the outer ring surrounds the primary in circular orbits for which no radial velocity components in the line of sight are expected. However, if the outer ring were to move along an eccentric orbit around the primary, finite radial velocity components in the line of sight would be present. Such an elliptical outer disk would reveal a quasi-stationary radial component of the orbital velocity ($\gamma \neq 0$), if the alignment of the line of apsides toward the observer changes slowly compared to time scale P_0. In particular, if γ varies with beat period P_b, the line of apsides would complete one revolution in the time interval P_b (in the observer's frame of reference), which corresponds to one revolution per time interval P_s in the binary's internal coordinate system. During time interval P_s, the gas stream from L_1 migrates once over all parts of the elliptical disk. When it arrives near periastron, the maximal potential energy is released in the stream-disk impact region, which leads to a light maximum within the time interval P_s, i.e., a superhump. At the opposite phase, when the gas stream impacts near the disk apastron, a light minimum is expected. Evidently such a configuration gives a natural explanation for superhumps. Figure 9 illustrates this effect, showing the binary configuration during both spectroscopic observing runs at the moment $\phi_s = 0$, i.e., at superhump maximum. The positions of primary and secondary toward the observer are defined by the orbital phase at $\phi_s = 0$; the angle between line of sight and semimajor axis of the elliptical disk is given (approximately) by the sign of γ in each spectroscopic run. Figure 9 demonstrates that, during both runs, the gas stream actually impacts near the disk periastron at superhump maximum ($\phi_s = 0$).

The remaining superoutburst properties can be understood within this model as well. Positive $O-C$ deviations of the eclipses (§§ IIa, IVa[iv]) are expected, since the gas stream always impacts at the disk portion which follows the primary. $O-C$ oscillations with beat period P_b (§ IVa[iv]) are due to the periodically changing position of the apparent radiation center within the eccentric disk. The correlation between Balmer absorption strength and continuum intensity (§ IIIb[ii]) could result from a higher density and temperature of the orbiting disk material near periastron, as compared to other parts of the ring. It is also evident that the superhump amplitude does not depend on the orbital inclination (§ IVa[ii]) since it reflects intrinsic flux variations. However, the spectrum of an SU UMa star with lower inclination will look different because the eccentric ring will no longer cross the line of sight toward the white dwarf and central disk. The very broad and flat Balmer absorption (§ IVa[v]) may arise in the reversing layer over the entire disk, from material which, in the case of higher inclination, contributes to the line emission.

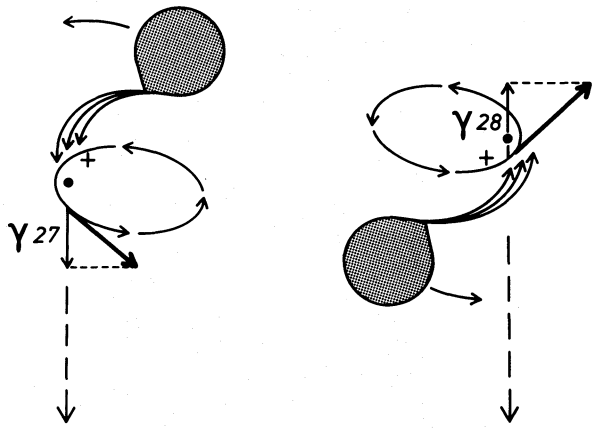

FIG. 9.—Relative positions of binary components, eccentric disk, and gas stream with respect to the line of sight in 1978 March 27/28 (*left*) and March 28/29 (*right*), in both cases at the moment of superhump maximum ($\phi_s = 0$). The dot refers to the primary (white dwarf); the gray area, to the secondary; the cross, to the center of gravity. The orbital velocity of the eccentric ring in the line of sight is indicated by a broad arrow, its radial component (observable as γ_{27} and γ_{28}, respectively) by a narrow arrow. The dashed arrows mark the direction toward the observer. Note that the gas stream impacts the eccentric ring near periastron in both spectroscopic observing runs. Ring size and eccentricity are slightly exaggerated.

Photometric and spectroscopic data of Z Cha and of other dwarf novae in superoutburst are, therefore, consistent with an eccentric outer disk. More quantitative conclusions about this disk will be given in the next section, in context with the physical reasons for its formation.

Instead of *radial components* of an orbital disk motion around the primary, one may consider *true radial motions* of the disk material, as an alternative hypothesis in order to explain $\gamma \neq 0$. In principle, accretion models of dwarf nova outbursts offer this possibility, since they require infalling disk material toward the primary. In this case, however, one would always expect $\gamma > 0$ during outburst. Only γ_{28} fulfils this conditions (cf. § IIIb[v]) while $\gamma_{27} < 0$ (§ IIIb[vi]). Also WZ Sge reveals γ-values with both signs during outburst (cf. § IVb). Simple accretion clearly is inadequate. Rather a disk pulsation mechanism would be required which implies relatively long lasting inward and outward disk motion, alternating in a time scale of the beat period P_b. Since P_b exceeds the time necessary to cross the primary's Roche lobe with velocity γ_{27} by a factor ~ 100, this model would imply a large mass flow from the binary system, whenever $\gamma < 0$. Although there is no *a priori* reason to abandon this idea without further study, such a disk pulsation seems improbable due to the long pulsation period required, and due to the lack of theoretical as

well as further observational evidence for disk pulsation in general.

V. ON THE ORIGIN OF SUPERMAXIMA

For the following discussion it is assumed that dwarf nova eruptions are generally caused by a sudden gravitational energy release due to intermittent accretion of disk material onto the white dwarf (Osaki 1974; Paczyński 1978). This refers to all dwarf nova eruptions of U Gem, SS Cyg, and Z Cam subtypes (all with $P_0 > 3^h$), as well as to the short eruptions of SU UMa type dwarf novae ($P_0 \lesssim 2^h$). In all these cases the mass transfer rate from L_1 remains unaffected by the eruption. In quiescence, the transferred mass is accumulated in a torus whose structure could be similar to Madej and Paczyński's (1977) model. However, a smaller optical thickness is required in order to explain the narrow absorption lines in the quiescence spectrum of Z Cha (cf. § II*a*). Short eruptions of Z Cha and other dwarf novae begin with a sudden collapse of the torus, due to an unknown disk instability, with subsequent brightening of the central parts of the disk and accretion onto the white dwarf. Possibly part of the outer disk has to be ejected in order to remove the excess of angular momentum. But this is not entirely clear since Papaloizou and Pringle (1977) showed that the angular momentum can also be transferred from disk rotation into the orbital motion of the two stars, via tidal torques.

A superoutburst always begins as a normal dwarf nova eruption, i.e., with the collapse of the outer disk. Therefore, the rise to supermaximum does not differ from that to short eruptions (cf. § IV*a*[i]). Near or just after light maximum, however, there occurs a sudden mass transfer push through L_1, roughly of the same type as studied by Bath (1975). For the model suggested here it is important that this "push" is restricted to a very short time ($\lesssim 10^3$ s). The transferred matter will pass the primary, advance to a point near the primaries Roche lobe and, when returning near the primary, cross the incident stream line closing an elliptical orbit. The duration of mass transfer has to be shorter than the time necessary to complete this orbit: only so the returning stream will not impact the incident stream (which by then has already ceased), enabling the eccentric orbit to be maintained for many revolutions. The undisturbed trajectory of a stream ejected in L_1 was calculated by Lubow and Shu (1975, Fig. 4*a*), an ellipse-like orbit with the apastron near the Roche lobe. If the periastron distance exceeds the disk radius at outburst (which, in any case, will be smaller than the outer disk limit in quiescence as determined in § II*b*), the transferred material remains undisturbed along its entire orbit (in a first approximation), and therefore maintains its orbit fixed in the observer's reference frame. However, the tidal interaction of the secondary will cause a slow rotation of the line of apsides, e.g., with period P_b which gives rise to the situation deduced from the observations in § IV*d*.

The reason for a sudden mass transfer "push" remains speculative at the moment. Apart from dynamical instabilities, as suggested by Bath (1975), one may consider the temporary alignment of two or more nonlinear *g*-mode oscillations of the secondary (Vogt 1980). Whatever trigger mechanism is assumed for the sudden mass transfer enhancement, it will be effective only if a short eruption takes place, probably due to the additional heating of the secondary's atmosphere around L_1 by the erupting disk. This would also explain why strongly periodic mechanisms, such as *g*-mode pulsation, result in a rather roughly periodic repetition of supermaxima. Indeed, the trigger mechanism causes periodically repeating time intervals in which a mass transfer enhancement is possible. Only if a short eruption occurs during this critical time does it develop into a superoutburst. Therefore, SU UMa stars with frequent short eruptions (e.g., VW Hyi) show a better pronounced periodicity of supermaxima than those with rare short eruptions (e.g., Z Cha).

The further development of the supermaximum is dominated by the superhump phenomenon, i.e., by the periodically changing amount of potential stream energy released in collision with the eccentric disk ("superspot"). The disk eccentricity can be estimated from the requirement that the periastron distance r_p be larger than the diameter of the outbursting inner disk which, according to the photoelectric observations, is never totally eclipsed. This requirement leads to $r_p \approx \frac{1}{2} r_d$ where r_d is the outer disk radius at quiescence (cf. § II*b*). Assuming an apastron distance near the Roche lobe of the primary, one derives $e \approx 0.6$. The resulting mean orbital velocity of ~ 800 km s^{-1} and maximal radial velocity components of ± 300 km s^{-1} are in good agreement with the observed values of γ_{27} and γ_{28}. An eccentricity $e \approx 0.6$ implies that the potential energy of the gas stream released in the superspot will vary by a factor ~ 4 within time interval P_s. Therefore, the observed superhump variations (~ 0.2 mag) are seen over a background of constant brightness (inner disk), which exceeds the mean intensity of the superspot by a factor ~ 10. At quiescence, the hot spot contributes $\sim 36\%$ of the total light (Smak 1979), i.e., a factor ~ 20 less than the total light at supermaximum in 1979 March 29/30. Therefore, the superspot is only a factor ~ 2 brighter than the hot spot in quiescence. These results are quite uncertain due to the unknown differential bolometric corrections which have to be applied to spot and disk in both states of activity. In any case, the similar spot brightness in quiescence and in eruption implies a similar mass transfer rate; i.e., after the sudden "push" the mass transfer rate immediately decreases to about twice the quiescent value.

The mass of the eccentric ring, i.e., the mass transferred during the sudden "push," can be estimated from the outburst light curve characteristics as given by Bateson (1978). In our model no accretion takes place during quiescence. Therefore, the material transferred in quiescence (i.e., in 93^d between two subsequent outbursts) is accreted within $\sim 1^d.2$, the typical duration of a short eruption. Assuming a transfer rate of $\sim 10^{16}$ g s^{-1} (Bath 1975), we derive an average accretion rate of 8×10^{17} g s^{-1} and a total mass of 8×10^{22} g accreted during a short eruption. Supermaxima are, in average, 0.6 mag brighter than normal outbursts, and last $\sim 9^d$; their total energy output exceeds that of normal eruptions by a factor ~ 13. If this excess luminosity is caused by additionally accreted matter, a total of 1×10^{24} g is required. Since the current mass transfer rate in supermaximum resembles the quiescence rate 10^{16} g s^{-1}, the additional mass must be taken from the eccentric ring, probably due to the interaction between inner disk and ring near periastron. This implies a total mass of the ring of the order 10^{24} g, and a rather large mass transfer rate of $\sim 10^{21}$ g s^{-1} during the sudden "push." Afterwards, the eccentric outer ring refuels permanently the inner disk near periastron, maintaining a quasi–steady-state accretion until the material of the eccentric disk is used up. The lifetime of the eccentric ring actually is limited by these accretion losses, and not by the interaction with the gas stream from L_1: after the "push," only $\sim 1\%$ of the total mass of the ring is transferred through L_1 in the course of the entire supermaximum. Therefore, the impacting gas stream gives rise to superhumps, but will not considerably disturb the eccentric orbits of the ring material.

Evidently, these estimates indicate just orders of magnitude of all derived quantities. Bolometric corrections were neglected. Furthermore, it remains uncertain whether all transferred matter is actually accreted during outburst. Probably part of the matter will leave the system, especially during supermaximum when the eccentric disk extends near the primary's Roche lobe. There is no direct observational evidence for mass loss, except the stationary Balmer emission of WZ Sge in outburst (cf. § IV*b*), which, however, seems not to be present in Z Cha during supermaximum.

VI. CONCLUSIONS

Z Cha certainly is one of the few touchstones for dwarf nova studies. The aim of this paper was to present crucial photometric and spectroscopic observations, especially in the superoutburst state, and to interpret these data taking into account also the properties of other SU UMa type dwarf novae during supermaximum. Previously suggested models have failed to give a consistent picture. Among other problems, they do not account for the shifting γ-velocities of the narrow Balmer absorption, displayed clearly in Z Cha and WZ Sge during superoutburst. This fact forced us to assume an eccentric disk which is formed by a sudden mass transfer enhancement of very short duration ($\sim 10^3$ s). Bath's (1975) dynamical instabilities of the secondary near the inner Lagrangian point offer this possibility, which, however, seems to be restricted to a particular moment near maximum brightness of the outburst. Furthermore, it was assumed that the eruption activity of dwarf novae in general, including short eruptions of SU UMa stars, is triggered by disk instabilities, resulting in a collapse of the outer disk when the outburst starts (Osaki 1974). Based on these two assumptions a consistent picture was developed which is able to explain the occurrence of two distinct types of eruptions for SU UMa stars, the superhump phenomenon, the eclipse timing and shape in outburst, relative strength of emission and absorption features in the spectrum (including their changes with orbital phase), and the observed radial velocity variations. The mass transfer rates were roughly estimated. The total mass of the eccentric disk turned out to be of the order of 10^{24} g. A quantitative elaboration of the model requires more complete observations, covering all states of a supermaximum of Z Cha, including rise and decline, and an extension of the wavelength range toward the UV (in order to derive the bolometric corrections). Also some theoretical aspects deserve further study, e.g., the apsidal rotation period of an eccentric disk in a close binary system, and the trigger mechanism for the suddenly increased mass transfer.

It is a pleasure to thank Drs. Michéle Klutz and Jean Surdej for their cooperation in performing *UBV* measurements of Z Cha, and in ceding valuable observing hours at the ESO 50 cm telescope, which enabled me to determine the superhump period. I also thank Frank M. Bateson who kindly placed to my disposal numerous visual observations of Z Cha, performed by members of the Royal Astronomical Society of New Zealand, Variable Star Section.

REFERENCES

Bailey, J. 1979, *M.N.R.A.S.*, **187**, 645.
Bateson, F. M. 1978, *M.N.R.A.S.*, **184**, 567.
_____. 1980, private communication.
Bateson, F. M., Jones, A. F., and Stranson, I. 1966, *Charts for Southern Variables*, Series 3.
Bath, G. T. 1975, *M.N.R.A.S.*, **171**, 311.
Bath, G. T., Evans, W. D., Papaloizou, J., and Pringle, J. E. 1974, *M.N.R.A.S.*, **169**, 447.
Bohusz, E., and Udalski, A. 1979, *Inf. Bull. Var. Stars*, No. 1583.
Breysacher, J., and Vogt, N. 1980, *Astr. Ap.*, **87**, 349.
Brosch, N., Leibowitz, E. M., and Mazeh, T. 1980, *Ap. J. (Letters)*, **236**, L29.

Crampton, D., Hutchings, J. B., and Cowley, A. P. 1979, *Ap. J.*, **234**, 182.
Fabian, A. C., Pringle, J. E., Whelan, J. A. J., and Bailey, J. A. 1979, in *IAU Colloquium 46, Changing Trends in Variable Star Research*, ed. F. M. Bateson *et al.* (Hamilton, New Zealand), p. 65.
Gilliland, R. L., and Kemper, E. 1980, *Ap. J.*, **236**, 854.
Grossmann, A. S., Hays, D., and Graboske, H. C., Jr. 1974, *Astr. Ap.*, **30**, 95.
Haefner, R., Schoembs, R. and Vogt, N. 1979, *Astr. Ap.*, **77**, 7.
Kippenhahn, R., and Thomas, H. C. 1965, *Landolt-Börnstein, Numerical Data and Functional Relationships in Science and Technology*, Group VI, Vol. **1**, ed. H. H. Voigt (Berlin: Springer), p. 485.
Knoechel, G., and Vogt, N. 1981, in preparation.
Krzeminski, W., and Kraft, R. P. 1964, *Ap. J.*, **140**, 921.
Krzeminski, W., and Vogt, N. 1981, in preparation.
Lubow, S. H., and Shu, F. H. 1975, *Ap. J.*, **198**, 383.
Madej, J., and Paczyński, B. 1977, in *IAU Colloquium 42, The Interaction of Variable Stars with their Environment*, ed. R. Kippenhahn *et al.* (Veröff. Remeis-Sternwarte Bamberg), Vol. **11**, No. 121, p. 313.
Meyer, F. 1979, in *IAU Colloquium 53, White Dwarfs and Variable Degenerate Stars*, ed. H. M. Van Horn and V. Weidemann (Rochester: University of Rochester), p. 528.
Mumford, G. S. 1969, *IAU Inf. Bull. Var. Stars*, No. 337.
Ortolani, S., Rafanelli, P., Rosino, L., and Vittone, A. 1980, *Astr. Ap.*, **87**, 31.
Osaki, Y. 1974, *Pub. Astr. Soc. Japan*, **26**, 429.
Paczyński, B. 1971, *Ann. Rev. Astr. Ap.*, **9**, 183.
_____. 1978, in *Nonstationary Evolution of Close Binaries*, ed. A. N. Żytkow (Warsawa), p. 89.
Papaloizou, J., and Pringle, J. E. 1977, *M.N.R.A.S.*, **181**, 441.
Papaloizou, J., and Pringle, J. E. 1978, *Astr. Ap.*, **70**, L65.
_____. 1979, *M.N.R.A.S.*, **189**, 293.
Patterson, J. 1978, Ph.D. thesis, University of Texas at Austin.
Rayne, M. W., and Whelan, J. A. J. 1981, *M.N.R.A.S.*, **196**, 73.
Ritter, H. 1980, *Astr. Ap.*, **86**, 204.
Robinson, E. L., Nather, R. E., and Patterson, J. 1978, *Ap. J.*, **219**, 168.
Schoembs, R., and Vogt, N. 1980, *Astr. Ap.*, **91**, 25.
_____. 1981, *Astr. Ap.*, **97**, 185.
Smak, J. 1979, *Acta Astr.*, **29**, 309.
Vogt, N. 1976, in *IAU Symposium 73, Structure and Evolution of Close Binary Systems*, ed. P. Eggleton *et al.* (Dordrecht: Reidel), p. 147.
_____. 1977, in *IAU Colloquium 42, The Interaction of Variable Stars with their Environment*, ed. R. Kippenhahn *et al.* (Veröff. Remeis-Sternwarte Bamberg), Vol. **11**, No. 121, p. 227.
_____. 1979*a*, *IAU Circ.*, No. 3357.
_____. 1979*b*, *Mitt. Astr. Ges.*, **45**, 158.
_____. 1980, *Astr. Ap.*, **88**, 66.
Vogt, N., Schoembs, R., Krzeminski, W., and Pedersen, H. 1981, *Astr. Ap. (Letters)*, **94**, L29.
Walker, M. F., and Bell, M. 1980, *Ap. J.*, **237**, 89.
Warner, B. 1974, *M.N.R.A.S.*, **168**, 235.
_____. 1976, in *IAU Symposium 73, Structure and Evolution of Close Binary Systems*, ed. P. Eggleton *et al.* (Dordrecht: Reidel), p. 85.
Webbink, R. F. 1979, in *IAU Colloquium 46, Changing Trends in Variable Star Research*, ed. F. M. Bateson *et al.* (Hamilton, New Zealand), p. 102.
Whelan, J. A. J., Rayne, M. W., and Brunt, C. C. 1979, in *IAU Colloquium 46, Changing Trends in Variable Star Research*, ed. F. M. Bateson *et al.* (Hamilton, New Zealand), p. 39.

NIKOLAUS VOGT: European Southern Observatory, Casilla 16317, Santiago 9, Chile